Examination of cobalt, nickel, copper and zinc(II) complex geometry and binding affinity in aqueous media using simple pyridylsulfonamide ligands†

Aileen Congreve, Ritu Kataky, Mark Knell, David Parker,* Horst Puschmann, Kanthi Senanayake and Lisa Wylie

Department of Chemistry, University of Durham, South Road, Durham, UK DH1 3LE. E-mail: david.parker@dur.ac.uk

The sixteen neutral ML_2 complexes of Co, Ni, Cu and Zn(II) with the *p*-toluenesulfonamide and trifluoromethylsulfonamide derivatives of 2-aminomethylpyridine (L^1, L^2) and its 6-Me homologue (L^3, L^4) have been characterised by low temperature X-ray crystallography (100–120 K). Complexes of Co and Zn invariably adopted a distorted tetrahedral geometry and whilst Cu(II) complexes of L^2, L^3 and L^4 also took up a distorted tetrahedral geometry, that with L^1 was square planar. A database survey of the distortion from limiting tetrahedral/square planar geometry has been carried out, aided by a simple geometric analysis. The trifluoromethylsulfonamide ligands (L^2 and L^3) were less basic, *e.g.* log K_1 7.51(3) for L^2 *vs.* 12.23(6) for L^1 (80% MeOH/H_2O) and afforded a weaker ligand field, exemplified by the position of the visible d–d transition in Cu(II) complexes and the ease of reduction of the Cu(II) centre: $E_{\frac{1}{2}}$ values (MeCN *vs.* Ag/AgCl) are -430, -137, $+55$ and -240 mV for Cu(L^1)$_2$, Cu(L^2)$_2$, Cu(L^3)$_2$ and Cu(L^4)$_2$. Ligand protonation and stepwise formation constants have been measured for L^1–L^3 and derived species distribution diagrams reveal that for complexes with L^2 and L^3, the predominant species present at pH 7.4 when zinc was in the nanomolar range was ZnL_2.

The binding of the Zn ion in aqueous media has attracted attention recently in three different areas of chemistry. Firstly, stimulated by the need to probe the biological rôle of kinetically labile zinc[1] in synaptic neurotransmission[2] and excitotoxicity,[3,4] a range of luminescent zinc probes has been devised in which a chromophore or fluorophore is integrated into the ligand structure.[5–11] Such ligands need to bind the zinc ion with high affinity in the physiological pH range and examples have been reported with micromolar,[11] nanomolar[4,5,8] or sub-picomolar[12] apparent dissociation constants. Secondly, more lipophilic zinc binding ligands have been sought that allow the selective extraction of the zinc ion from acidic aqueous media into a non-polar organic phase. Examples have included aza-carboxylates and phosphinates[13,14] in which a tetrahedral binding geometry is imposed on the zinc by ligand design. Finally, as a consequence of the pivotal role of zinc in gene transcription and metalloenzyme function,[1,15] a great deal of work has been directed at devising zinc-binding ligands that inhibit enzyme function and hence may allow development of therapeutic agents. In just one example, inhibition of carbonic anhydrase activity has been observed with a series of sulfonamide ligands which bind to zinc *via* nitrogen.[16] Thus, various thiadiazole sulfonamides[17,18] are active inhibitors, as is the simple example trifluoromethylsulfonamide.[19] Such work has led to the parallel development of sulfonamide probes for the fluorescence anisotropy detection of zinc with a carbonic-anhydrase-based biosensor.[20]

We set out to compare the co-ordination chemistry of the series of simple pyridyl-sulfonamide ligands L^1–L^4. The introduction of the α-methyl substituent was expected to sterically inhibit formation of a square planar ML_2 complex. The differing sulfonamide substituents (CF_3 *vs.* tosyl) alter the electron donating ability of the sulfonamide nitrogen. Furthermore, the lower protonation constants of trifluoromethylsulfonamides (*ca.* 7.5) *vs.* arylsulfonamides (*ca.* 12) was expected to inhibit protonation of the ML and ML_2 complexes and enhance complex stability at ambient pH. Our aim was to identify a model ligand system from this series capable of forming a well-defined neutral complex with zinc under ambient pH conditions, when the Zn concentration is of the order of 100–0.1 nM. Such a system could then form the basis of new luminescent or MR probes.
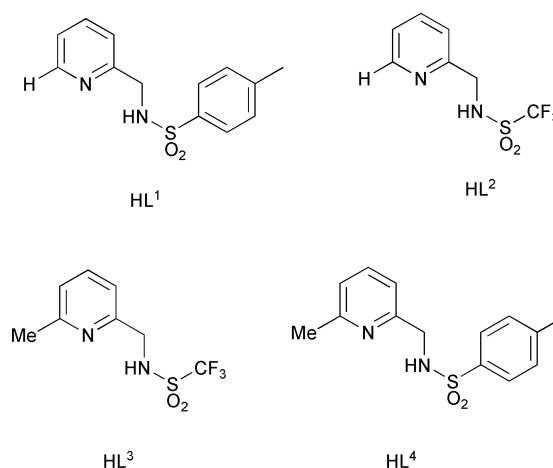
DOI: 10.1039/b206279h

Experimental

Solvents were dried from an appropriate drying agent where required using standard procedures. Water was purified by the "Purite$_{STILL}$ plus" system. Thin layer chromatography was carried out using fluorescent (254 nm) silica plates (Merck Art 5554). Preparative column chromatography was carried out using silica (Merck silica gel 60, 230–400 mesh). Mass spectra (ES MS) were recorded using a VG II Platform spectrometer (Fisons Instruments) with methanol as the carrier solvent. FAB spectra were recorded by the EPSRC Mass Spectrometry Service at the University of Wales at Swansea. NMR spectra were recorded on a Varian Unity 300 spectrometer at 299.91 MHz (^{1}H) and 75.41 MHz (^{13}C) or a Varian Mercury 200 spectrometer at 199.99 MHz (^{1}H), 50.29 MHz (^{13}C) or 188.18 MHz (^{19}F) or a Bruker AC250 spectrometer at 62.90 MHz (^{13}C). Chemical shifts are quoted with reference to the residue residual protonated solvent and are given in ppm with coupling constants in Hz. Infra-red spectra were recorded on a Perkin-Elmer FT-IR 1720X spectrometer with GRAMS Analyst operating software. Ultraviolet absorbance spectra of the complexes (1 mM) were recorded in acetonitrile on a Unicam UV2 spectrometer operating with Vision software. Melting points were determined on a Reichert-Koefler block melting point apparatus and are uncorrected. Cyclic voltammetry of the complexes (0.001 M) was carried out in a background electrolyte of tetrabutylammonium perchlorate, TBAP (0.01 M), in acetonitrile controlled with an EG&G PARC Model 273 potentiostat. Computer control and data storage were achieved using EG&G PARC Model 270 Research Electrochemistry software. The auxiliary electrode was made of platinum foil, (area 1 cm^2), connected to a copper wire mounted in a glass body. The working electrode was made of glassy carbon, purchased from BAS. The reference electrode was a non-aqueous silver/silver chloride electrode, self-assembly kit, purchased from BAS. The electrodes were mounted in a circular Teflon cap and placed in a cylindrical cell (diameter 20 mm, length 65 mm), which was filled with 10 ml of the desired solution and purged with argon. The cell assembly was placed inside a Faraday cage to eliminate stray field interference.

Potentiometric analyses were carried out using an apparatus described previously.[21,22] The stepwise protonation and metal formation constants were evaluated by analysis of data acquired using a computer-controlled alkalimetric titration at 298 K (water-jacketed titration cell), using a calibrated Corning pH glass electrode, under an argon atmosphere. To solutions of the ligand (typically 2 mM) in tetramethylammonium nitrate solution (0.1 M, 80% aqueous methanol) was added a fixed volume of 1.0 M HCl solution (Analar) to give the hydrochloride salt. The titrant was degassed sodium hydroxide solution (0.05 M, 80% MeOH/water) and the burette function (volume increments, total volume delivered and the time interval allowed for equilibration between each reading) was computer controlled allowing smaller increments of titrant to be added towards the end-point. Titration data for protonation equilibria were collected between pH 3 and 11, typically acquiring 80 data points, used in the subsequent analysis. In measuring the metal complex formation constants, separate titrations were carried out at 1:1 and 1:2 metal/ligand ratios, and the pH range examined was from 3 to ca. 7.5, at which point formation of the metal hydroxide was visually discerned. Data were analysed using HYPERQUAD[23] and corrections to pKw were applied to allow for solvent composition.[24] Each of the metal salt hydrolysis constants used in the data analysis was taken from the IUPAC Stability Constants database Version 5.12, published by IUPAC and Academic Software, 2000. Values of protonation and metal complex formation constants, determined by iterative fitting in Hyperquad, refer to the mean of three independent titrations and gave satisfactory statistical parameters (σ ca. 2.5 to 3.5 and χ^2 of the order of 8 to 12).

Single crystal X-ray diffraction experiments were carried out using SMART CCD area detectors and graphite-monochromated Mo-Kα radiation. The structures were solved by direct methods and refined against F^2 of all data, using SHELXTL programs.[25] A summary of cell and refinement data is given in Table 1.

CCDC reference numbers 186296–186312. See http://www.rsc.org/suppdata/nj/b2/b206279h/ for crystallographic data in CIF or other electronic format.

Ligand synthesis

6-Methylpyridine-2-aldoxime was prepared as described in the literature.[26]

2-(p-Toluenesulfonylaminomethyl)pyridine. L^1. To a stirred solution of p-toluenesulfonyl chloride (3.43 g, 0.018 mmol) in pyridine (10 ml) cooled to −10 °C was slowly added (2-aminomethyl)pyridine (2.00 g, 0.018 mmol) in pyridine (5 ml). The resulting reaction mixture was stirred at −10 °C for 3 hours and was held at 5 °C overnight. The reaction mixture was

Table 1 Unit cell and crystallographic data for Zn, Cu, Ni and Co complexes of L^1–L^4

Complex	a/Å	b/Å	c/Å	α/°	β/°	γ/°	Volume/Å^3	System	Space group	Z	μ/mm^{-1}	T/K	R_{int} (%)	Rw (%)	R (%)
L^1	26.831(4)	5.958(1)	16.576(2)	90	99.967(3)	90	2610.1(6)	Monoclinic	$C2/c$	8	0.249	110	3.05	9.20	3.84
Zn(L^1)$_2$	30.505(2)	8.010(1)	27.309(1)	90	123.815(3)	90	5543.8(9)	Monoclinic	$C2/c$	8	1.081	100	8.30	10.94	4.83
Zn(L^2)$_2$	8.296(1)	9.721(1)	13.035(1)	93.193(4)	95.817(4)	107.145(4)	995.27(17)	Triclinic	$P\bar{1}$	2	1.529	100	2.06	6.64	2.72
Zn(L^3)$_2$	7.973(1)	9.432(1)	14.746(1)	81.984(1)	81.130(1)	81.744(10)	1076.38(5)	Triclinic	$P\bar{1}$	2	1.419	105	2.56	8.35	2.99
Zn(L^4)$_2$	28.129(1)	12.033(1)	16.726(1)	90	91.701(1)	90	5658.54(17)	Monoclinic	$I2/a$	8	1.057	120	2.48	6.65	2.69
Cu(L^1)$_2$	7.293(1)	17.089(1)	9.912(7)	90	99.176(4)	90	1219.56(15)	Monoclinic	$P2_1/c$	2	1.11	100	4.14	8.99	3.31
Cu(L^2)$_2$^{b}	9.04(5)	10.29(5)	20.70(5)	90	91.71(5)	90	1923(10)	Monoclinic	Pc	4	1.442	100	5.60	36.05	14.10
Cu(L^3)$_2$	10.450(1)	14.023(1)	15.197(1)	90	106.221(1)	90	2138.19(10)	Monoclinic	$P2_1/c$	4	1.301	105	5.26	8.17	3.45
Cu(L^4)$_2$	26.673(1)	14.539(1)	14.980(1)	90	102.051(1)	90	5680.9(3)	Monoclinic	$C2/c$	8	0.96	110	15.03	18.56	7.32
Ni(L^1)$_2$	7.335(1)	17.058(1)	9.822(1)	90	99.139(1)	90	1213.25(8)	Monoclinic	$P2_1/c$	2	1.015	120	5.46	20.24	6.99
Ni(L^2)$_2$	10.458(1)	16.052(2)	29.546(4)	90	90	90	4960.1(11)	Orthorhombic	$Pbca$	8	1.038	100	4.21	15.38	5.89
Ni(L^3)$_2$	7.936(1)	9.450(1)	14.716(1)	80.519(1)	80.609(1)	81.548(1)	1065.77(6)	Triclinic	$P\bar{1}$	2	1.191	100	2.42	9.33	3.36
Ni(L^4)$_2$	32.016(1)	11.932(4)	16.782(8)	90	118.86(2)	90	5615(4)	Monoclinic	$C2/c$	8	0.881	120	4.23	11.8	4.35
Co(L^1)$_2$	29.967(6)	7.977(1)	26.183(5)	90	121.349(5)	90	5345.2(17)	Monoclinic	$C2/c$	8	0.838	100	5.23	9.00	3.73
Co(L^2)$_2$	8.270(1)	9.801(1)	13.050(1)	93.015(1)	95.599(1)	108.418(1)	994.84(6)	Triclinic	$P\bar{1}$	2	1.158	110	3.19	9.47	3.69
Co(L^3)$_2$	8.000(1)	9.372(1)	14.736(1)	82.625(1)	81.527(1)	81.726(1)	1074.89(6)	Triclinic	$P\bar{1}$	2	1.076	100	2.90	9.25	3.59
Co(L^4)$_2$	32.449(1)	12.065(1)	16.738(1)	90	119.72(1)	90	5694.0(3)	Monoclinic	$C2/c$	8	0.790	110	5.26	11.7	3.82

^{a} Remaining solvent electron density was refined to 0.13 molecules of water. ^{b} These crystals were badly twinned, despite appearing perfectly well formed. Satisfactory anisotropic refinement was not possible.

poured onto crushed ice resulting in the precipitation of a yellow solid, which was removed by filtration and washed with water. The precipitate was dissolved in dichloromethane, dried (NaSO$_4$) and the solvent evaporated yielding pale yellow crystals (2.12 g, 45%), mp 76–77 °C; ^{1}H NMR (200 MHz, CD$_3$OD): δ_H 2.40 (s, 3H, CH$_3$), 4.15 (s, 2H, CH$_2$), 7.22–7.45 (4H, m, H3, H5, H3′, H5′), 7.69 (3H, m, H4, H4′, H6′), 8.37 (1H, d, J 4.4, H6); ^{13}C NMR (50.29 MHz, CDCl$_3$): δ_c 21.15 (Me), 47.47 (CH$_2$), 122.00 (C3 or C5), 122.32 (C3 or C5), 126.75 (C3′ + C5′), 129.29 (C2′ + C6′), 136.72 (C4), 142.92 (C4′), 148.59 (C2), 155.34 (C1′); m/z ES$^+$: 546.7 (100%, 2M + Na), 284.5 (85%, M + Na); ν_{max} (KBr)/cm^{-1} 3250 (ν NH), 1599 (ν py), 1574 (ν py), 1441 (ν py), 1385 (δ NH), 1329 (ν_a SO$_2$), 1165 (ν_s SO$_2$), 1111 (δ CH), 1089 (δ CH), 1007, 901 (ν N–S), 763 (δ py), 662 (γ NH), 543 (δ SO$_2$); Found: C, 57.12; H, 5.58; N, 10.25. C$_{13}$H$_{14}$N$_2$O$_2$S.0.5H$_2$O requires C, 57.54; H, 5.57; N, 10.32%.

2-(Trifluoromethylsulfonylaminomethyl)pyridine L^2. Under anhydrous conditions in an argon atmosphere, a solution of (2-aminomethyl)pyridine (0.64 g, 5.93 mmol) in anhydrous pyridine (5 ml) at −40 °C was added dropwise, over 10 minutes, to a stirred solution of trifluoromethanesulfonyl chloride (1.0 g, 5.93 mmol) in pyridine (10 ml) at −40 °C. The resulting bright yellow reaction mixture was stirred at −40 °C for 2 hours and kept at 5 °C overnight. The mixture was poured slowly onto crushed ice and stirred. The precipitate that formed was separated by filtration and washed with water. This precipitate was dissolved in dichloromethane (50 ml), washed with water (2 × 25 ml) and the organic phase was dried (MgSO$_4$), filtered and evaporated under reduced pressure to give a solid which was recrystallised from ethyl acetate and hexane to yield pale brown crystals (0.72 g, 50%), mp 80–84 °C; ^{1}H NMR (300 MHz, CDCl$_3$): δ_H 4.49 (2H, s, CH$_2$), 7.24 (2H, m, H3 + H5), 7.69 (1H, t of d, J 1.8, 7.8, H4), 8.46 (1H, d, J 5.1, H6); ^{13}C NMR (50.3 MHz, CDCl$_3$): δ_C 48.05 (CH$_2$), 123.10 (C2), 123.87 (C4), 138.20 (C5), 149.30 (C6), 154.47 (q, CF$_3$); ^{19}F NMR (188 MHz, CD$_3$CN): δ_F −79.44 (s, CF$_3$); m/z (ES$^+$): 263 (100%, M + Na$^+$), 241 (20%, M + H$^+$); ν_{max} (KBr)/cm^{-1} 1601 (ν py), 1434 (ν py), 1379 (δ NH), 1367 (ν_a SO$_2$), 1176 (ν_s SO$_2$), 1143 (δ CH), 1087 (δ CH), 599 (γ NH); Found: C, 35.30; H. 3.01; N. 11.52. C$_7$H$_7$N$_2$O$_2$SF$_3$ requires C. 35.00; H. 2.94; N. 11.66%.

2-Aminomethyl-6-methylpyridine. 10% Pd/C (0.114 g) was added to 6-methylpyridine-2-aldoxime (1.102 g, 8.09 mmol) dissolved in absolute ethanol (60 ml). The mixture was hydrogenated in a Parr hydrogenation apparatus at room temperature under 40 psi H$_2$ for 4 hours. The mixture was filtered through celite, which was washed thoroughly with ethanol and dichloromethane, the solvent was evaporated under reduced pressure to yield a clear colourless oil (0.915 g, 93%); ^{1}H NMR (200 MHz, CDCl$_3$): δ_H 2.47 (3H, s, CH$_3$), 3.87 (2H, s, CH$_2$), 6.93–7.08 (2H, m, H3, H5), 7.47 (1H, t, J 7.6, H4); ^{13}C NMR (200 MHz, CDCl$_3$): δ_C 24.56 (CH$_3$), 47.85 (CH$_2$), 118.35 (C5), 119.43 (q, C6), 121.61 (C3), 137.09 (C4), 158.12 (C2); m/z (ES$^+$): 122.9 (100%, MH$^+$).

2-(p-Toluenesulfonylaminomethyl)-6-methylpyridine L^4. To a stirred solution of p-toluenesulfonyl chloride (192 mg, 1.0 mmol) in pyridine (0.6 ml) cooled to −10 °C was slowly added a solution of 2-aminomethyl-6-methylpyridine (123 mg, 1.0 mmol) in pyridine (1 ml). The resulting yellow reaction mixture was stirred at −10 °C for 3 hours and was held at 5 °C overnight. The reaction mixture was poured onto crushed ice, which was allowed to melt resulting in the formation of an oil. A precipitate formed upon scratching. The solid was removed by filtration, dissolved in dichloromethane (5 ml) and washed with water (2 × 5 ml). The organic phase was dried (MgSO$_4$), filtered and evaporated under reduced pressure to

yield a yellow oil which was crystallised from ethanol and water (1%) to form a white solid (0.53 g, 53%); mp 83–84 °C; ^{1}H NMR (200 MHz, CDCl$_3$): δ_H 2.38 (3H, s, CH$_3$), 2.46 (3H, s, CH$_3$), 4.18 (2H, d, J 5.2, CH$_2$), 5.92 (1H, s, NH), 6.97 (2H, t, J 8.4, H3, H5), 7.22 (2H, d, J 7.8, H3′, H5′), 7.47 (1H, t, J 7.8, H4), 7.72 (2H, d, J 6.6, H2′, H5′); ^{13}C NMR (50.3 MHz, CDCl$_3$): δ_c 21.37 (Me), 24.02 (Me), 47.35 (CH$_2$), 118.74 (C4′), 121.94 (C1′), 127.08 (C3′ + C5′), 129.45 (C2′ + C6′), 136.63 (q, C6), 136.96 (C2), 143.17 (C3), 154.09 (C4), 157.68 (C2); m/z ES$^+$: 574.7 (25%, 2M + Na$^+$), 298.7 (100%, M + Na$^+$); ν_{max} (KBr)/cm^{-1} 1599 (ν py), 1458 (ν py), 1325 (ν_a SO$_2$), 1160 (ν_s SO$_2$), 1090 (δ CH), 816, 662 (γ NH), 551 (δ SO$_2$). Found: C, 60.57; H, 5.77; N, 10.39. C$_{13}$H$_{14}$N$_2$O$_2$S requires C, 60.85; H, 5.84; N, 10.14%.

2-(Trifluoromethanesulfonylaminomethyl)-6-methylpyridine L^3. Under anhydrous conditions in an argon atmosphere, a cooled solution of 2-aminomethyl-6-methylpyridine (0.45 g, 3.69 mmol) in anhydrous pyridine (2.4 ml) was added slowly to a stirred solution of trifluoromethanesulfonyl chloride (0.62 g, 3.69 mmol) in anhydrous pyridine (6.6 ml), which had been cooled to −40 °C. The resulting yellow solution was stirred at ∼−40 °C for two hours then kept at −18 °C overnight before being added slowly to crushed ice. The ice was stirred and allowed to melt resulting in the formation of a green precipitate, which was filtered off under suction. This precipitate was dissolved in dichloromethane (10 ml), washed with water (2 × 10 ml), the combined organic phase was dried (MgSO$_4$), filtered and the solution evaporated under reduced pressure to yield a yellow oil. The aqueous phase was extracted with dichloromethane (3 × 50 ml), the combined organic extracts were dried (MgSO$_4$), filtered and evaporated under reduced pressure to yield a yellow oil which was purified by flash column chromatography (SiO$_2$, 1:1 ethyl acetate:hexane). Clear crystals formed on the evaporation of the reduced eluting solvent (0.25 g, 30%), mp 73–74 °C. ^{1}H NMR (200 MHz, CDCl$_3$): δ_H 2.47 (3H, s, CH$_3$), 4.53 (2H, s, CH$_2$), 7.08 (2H, t, J 7, H3, H5), 7.61 (1H, t, J 7.8, H4); ^{13}C NMR (50.3 MHz, CDCl$_3$): δ_C 12.60 (CH$_3$), 47.80 (CH$_2$), 116.72 (q, C6), 119.49 (C5), 123.17 (C3), 137.64 (C4), 152.77 (C2), 158.34 (CF$_3$); ^{19}F NMR (188 MHz, CDCl$_3$): δ_F −77.70 (s, CF$_3$); m/z (ES$^+$): 255 (100%, MH$^+$); ν_{max} (KBr)/cm^{-1} 1606 (ν py), 1369 (ν_a SO$_2$), 1191 (ν_s SO$_2$), 1145 (δ CH), 1069 (δ CH), 611 (γ NH); Found: C, 37.73; H. 3.55; N. 10.91. C$_8$H$_9$N$_2$O$_2$SF$_3$ requires C. 37.80; H. 3.57; N. 11.02%.

Synthesis of metal complexes

The following are representative methods. Full details of remaining complexes are given in the ESI.†

Zn(C$_{13}$H$_{13}$N$_2$O$_2$S)$_2$ [Zn(L^1)$_2$]. 2-(p-Toluenesulfonylaminomethyl)pyridine L^1 (72 mg, 0.27 mmol) and zinc acetate (30 mg, 0.14 mmol) were dissolved in methanol (6 ml), and the resulting solution was heated under reflux for 6 hours. The solution was allowed to cool to room temperature. On standing overnight white crystals formed. These were collected by filtration and washed with cold methanol; mp 220 °C (decomp.); ^{1}H NMR (200 MHz, CD$_3$OD): δ_H 8.4 (2H, d, J 5, H6), 8.0 (2H, t, J 5, H4), 7.8 (4H, d, J 8, tos), 7.5 (4H, m, H5, H3), 7.2 (4H, d, J 8, tos), 4.4 (4H, s, CH$_2$), 2.3 (6H, s, Me); m/z (FAB): 587 (100%, ZnL$_2$), 431 (39%, ZnL$_2$ − tos), 325 (22%, ZnL), 263 (25%, LH); ν_{max} (KBr)/cm^{-1} 1611 (ν py), 1568 (ν py), 1442 (ν py), 1277 (ν_a SO$_2$), 1151 (ν_s SO$_2$), 1104 (δ CH), 1087 (δ CH), 970, 762 (δ py), 670 (γ NH), 560 (δ SO$_2$); Found: C, 52.53; H, 4.44; N, 9.40. Zn(C$_{13}$H$_{13}$N$_2$-O$_2$S)$_2$·0.5MeOH requires C, 52.69; H, 4.67; N, 9.27%.

Cu(C$_{13}$H$_{13}$N$_2$O$_2$S)$_2$ [Cu(L^1)$_2$]. 2-(p-Toluenesulfonylaminomethyl)pyridine L^1 (52 mg, 0.2 mmol) and copper acetate (40 mg, 0.2 mmol) were dissolved in methanol (10 ml) and heated under reflux for 18 hours. The solution was allowed to cool to

room temperature. On standing overnight blue and brown cubic crystals formed, these were collected by filtration and washed with cold methanol; mp 180–182 °C; m/z (FAB): 911 (11%, CuL$_3$), 650 (16%, Cu$_2$L$_2$), 608 (32%, CuL$_2$ + Na), 586 (100%, CuL$_2$) 325 (71%, CuL), 263 (22%, L + H); ν_{max} (KBr)/cm^{-1} 1609 (v py), 1570 (v py), 1447 (v py), 1276 (v_a SO$_2$), 1139 (v_s SO$_2$), 1106 (δ CH), 1085 (δ CH), 844, 813, 673 (γ NH), 557 (δ SO$_2$); λ_{max}(MeCN) 638 nm (ε 67 dm^3 mol^{-1} cm^{-1}); Found: C, 53.17; H, 4.46; N, 9.49. Cu(C$_{13}$H$_{13}$N$_2$O$_2$S)$_2$ requires C, 53.27; H, 4.47; N, 9.55%.

Ni(C$_{13}$H$_{13}$N$_2$O$_2$S)$_2$ [Ni(L^1)$_2$]. 2-(p-Toluenesulfonylaminomethyl)pyridine L^1 (66 mg, 0.25 mmol) was dissolved in methanol (2.5 ml), and neutralised with 0.1 M KOH solution (2.5 ml, 0.25 mmol), the solvent was evaporated under reduced pressure. The resulting brown oil was dissolved in methanol (7 ml) and nickel acetate (31 mg, 0.12 mmol) was added. The resulting clear green solution was heated under reflux with stirring for one hour. The solution was allowed to cool to room temperature. An orange precipitate formed overnight, which was collected by filtration and washed with cold methanol and water; mp 220 °C (decomp.); m/z (FAB): 603 (14%, NiL$_2$ + Na), 581 (63%, NiL$_2$), 425 (9%, NiL$_2$ − tos), 263 (100%, LH); ν_{max} (KBr)/cm^{-1} 1611 (v py), 1478 (v py), 1281 (v_a SO$_2$), 1139 (v_s SO$_2$), 1084 (δ CH), 681 (γ NH), 557 (δ SO$_2$); Found: C, 53.57; H, 4.68; N, 9.58. Ni(C$_{13}$H$_{13}$N$_2$O$_2$S)$_2$ requires C, 53.72; H, 4.51; N, 9.64%.

Co(C$_{13}$H$_{13}$N$_2$O$_2$S)$_2$ [Co(L^1)$_2$]. 2-(p-Toluenesulfonylaminomethyl)pyridine L^1 (131 mg, 0.5 mmol) was dissolved in methanol (5 ml), and neutralised with 0.1 M KOH solution (5 ml, 0.5 mmol) and the solvent evaporated under reduced pressure. The resulting brown oil was dissolved in methanol (10 ml) and cobaltous acetate hexahydrate (62 mg, 0.25 mmol) was added. The resulting dark purple solution was heated under reflux with stirring for seven hours. The solution was allowed to cool to room temperature. On standing purple

crystals formed after several days. These were collected by filtration and washed with cold methanol; mp 240 °C (decomp.); m/z FAB: 604 (37%, CoL$_2$ + Na), 582 (100%, CoL$_2$), 426 (39%, CoL$_2$ − tos), 320 (23%, CoL); ν_{max} (KBr)/cm^{-1} 1609 (v py), 1439 (v py), 1278 (v_a SO$_2$), 1145 (v_s SO$_2$), 1085 (δ CH), 947, 760 (δ py), 669 (γ NH), 559 (δ SO$_2$); λ_{max} (MeCN)/nm 513 and 579 (ε/dm^3 mol^{-1} cm^{-1} 302 and 291); Found: C, 53.20; H, 4.35; N, 9.51. Co(C$_{13}$H$_{13}$N$_2$O$_2$S)$_2$· 0.25MeOH requires C, 53.48; H, 4.61; N, 9.50%.
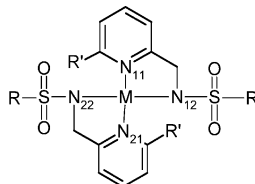
Results and discussion

Ligand and complex synthesis and X-ray structural characterisation

The ligands L^1–L^4 were prepared by reaction of the appropriate 2-(aminomethyl)pyridine with p-toluensulfonyl chloride or CF$_3$SO$_2$Cl in dry pyridine. The precursor 6-methyl-2-(aminomethyl)pyridine was prepared by reaction of the 6-aldehyde with hydroxylamine followed by reduction of the oxime[26] by catalytic hydrogenation over Pd/C. Formation of the ML$_2$ complex was undertaken by mixing two molar equivalents of ligand with one of the M(OAc)$_2$ salt in boiling methanol. On cooling, crystals of the neutral complex were deposited slowly—often over a period of several days. Each complex could be recrystallised from MeOH or EtOH. In the case of [Ni(L^1)$_2$] and [Co(L^1)$_2$] it was found necessary to form the potassium salt of the ligand, prior to complex formation.
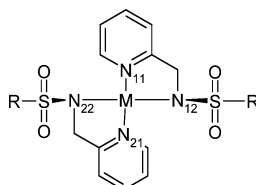
The structure of each of the sixteen neutral complexes has been determined by X-ray crystallography at 100–120 K (Tables 1–3; Fig. 1). The coordination geometry at Co(II) and Zn(II) was invariably a distorted tetrahedron, reflecting the minimisation of steric congestion, and for Co(II) the slightly favourable ligand field stabilisation effect. With Cu(II), the less sterically demanding ligand L^1 allowed formation of a square planar complex, whereas in complexes with L^2, L^3 and

**Table 2** Bond lengths, in Å, from the central metal ion to the coordinating nitrogens^a

				L^1	R = Ts,	R' = H
				L^2	R = CF$_3$,	R' = H
				L^3	R = CF$_3$,	R' = Me
				L^4	R = Ts,	R' = Me

Complex	M–N$_{11}$/Å	M–N$_{12}$/Å	M–N$_{21}$/Å	M–N$_{22}$/Å	Average M–N$_1$	Average M–N$_2$	Average M–N
[Zn(L^1)$_2$]	2.049(3)	1.942(3)	2.049(3)	1.956(3)	2.049	1.949	1.999
[Zn(L^2)$_2$]	2.023(2)	1.972(2)	2.043(2)	1.967(2)	2.033	1.969	2.001
[Zn(L^3)$_2$]	2.048(2)	1.965(2)	2.057(2)	1.966(2)	2.052	1.965	2.009
[Zn(L^4)$_2$]	2.050(7)	1.954(2)	2.089(2)	1.929(2)	2.069	1.941	2.004
[Cu(L^1)$_2$]	1.996(1)	1.998(1)	1.996(1)	1.998(2)	1.996	1.998	1.997
[Cu(L^2)$_2$]	1.949	1.939	1.998	1.916	1.974	1.928	1.951
[Cu(L^3)$_2$]	1.979(2)	1.973(2)	1.962(2)	1.969(2)	1.971	1.971	1.971
[Cu(L^4)$_2$]A	2.067(5)	1.920(5)	2.019(5)	1.944(5)	2.043	1.932	1.988
[Cu(L^4)$_2$]B	2.067(5)	1.914(5)	2.058(5)	1.918(5)	2.063	1.916	1.989
[Ni(L^1)$_2$]	1.924(5)	1.960(5)	1.924(5)	1.960(5)	1.924	1.960	1.942
[Ni(L^2)$_2$]	2.090(3)	2.123(3)	2.060(3)	2.099(3)	2.075	2.111	2.093
[Ni(L^3)$_2$]	2.021(2)	1.941(2)	2.028(2)	1.946(2)	2.025	1.944	1.9845
[Ni(L^4)$_2$]	2.040(2)	1.905(2)	2.014(2)	1.929(2)	2.027	1.917	1.972
[Co(L^1)$_2$]	2.031(2)	1.960(2)	2.037(2)	1.937(2)	2.034	1.949	1.9915
[Co(L^2)$_2$]	2.028(2)	1.962(2)	2.031(2)	1.968(2)	2.030	1.965	1.9975
[Co(L^3)$_2$]	2.040(2)	1.972(2)	2.035(2)	1.965(2)	2.038	1.969	2.0035
[Co(L^4)$_2$]	2.061(2)	1.934(2)	2.052(2)	1.960(2)	2.056	1.947	2.001

^{a} In CN = 4, mean ionic radii for Zn, Cu, Ni and Co(II) ions are 0.60, 0.57, 0.55 and 0.58 Å.[27] [Cu(L^4)$_2$]: This complex has two independent molecules in the unit cell.

Table 3 Bond angles, in degrees, between the central metal ion and the co-ordinating nitrogen atoms

L^1 R = Ts,   R' = H
L^2 R = CF$_3$,   R' = H
L^3 R = CF$_3$,   R' = Me
L^4 R = Ts,   R' = Me

Complex	N$_{11}$–M–N$_{12}$	N$_{11}$–M–N$_{21}$	N$_{11}$–M–N$_{22}$	N$_{12}$–M–N$_{21}$	N$_{12}$–M–N$_{22}$	N$_{21}$–M–N$_{22}$
[Zn(L^1)$_2$]	82.96(11)	122.40(10)	121.54(11)	117.73(11)	134.92(11)	82.59(10)
[Zn(L^2)$_2$]	83.12(6)	124.98(6)	124.75(6)	114.93(7)	131.99(7)	82.44(6)
[Zn(L^3)$_2$]	82.81(6)	113.20(6)	125.79(7)	123.81(7)	131.73(7)	83.32(6)
[Zn(L^4)$_2$]	82.8(2)	113.3(2)	129.8(3)	117.47(8)	134.01(8)	82.01(7)
[Cu(L^1)$_2$]	83.23(6)	180.00(8)	96.77(6)	96.77(6)	180.00(7)	83.23(6)
[Cu(L^2)$_2$]^a	82.3	147.3	105.6	105.6	154.7	81.0
[Cu(L^3)$_2$]	84.07(8)	150.57(9)	112.72(8)	103.40(8)	131.34(9)	83.92(8)
[Cu(L^4)$_2$]A	83.0(2)	140.66(19)	109.3(2)	107.2(2)	145.0(2)	84.2(2)
[Cu(L^4)$_2$]B	82.2(2)	128.82(19)	115.0(2)	110.6(2)	145.4(2)	82.7(2)
[Ni(L^1)$_2$]	94.4(2)	180.00(17)	85.6(2)	85.6(2)	180.0(3)	94.4(2)
[Ni(L^2)$_2$]	79.48(12)	91.01(12)	94.27(13)	97.31(13)	173.27(13)	80.18(13)
[Ni(L^3)$_2$]	82.13(7)	108.20(7)	124.26(8)	124.25(7)	137.32(8)	82.23(7)
[Ni(L^4)$_2$]	81.82(8)	110.69(8)	116.45(8)	133.00(8)	134.63(8)	81.64(7)
[Co(L^1)$_2$]	81.85(9)	122.08(9)	119.28(10)	119.19(10)	137.24(10)	82.59(9)
[Co(L^2)$_2$]	82.25(8)	125.16(8)	122.17(8)	116.01(9)	135.44(8)	81.83(8)
[Co(L^3)$_2$]	82.88(8)	115.13(8)	124.51(8)	127.66(9)	129.35(9)	82.12(8)
[Co(L^4)$_2$]	81.97(8)	114.45(8)	119.17(8)	128.57(8)	134.20(8)	81.94(7)

^{a} Twinned crystal. Structure of poor quality. ESD's are estimated at ±5 in the last digit.
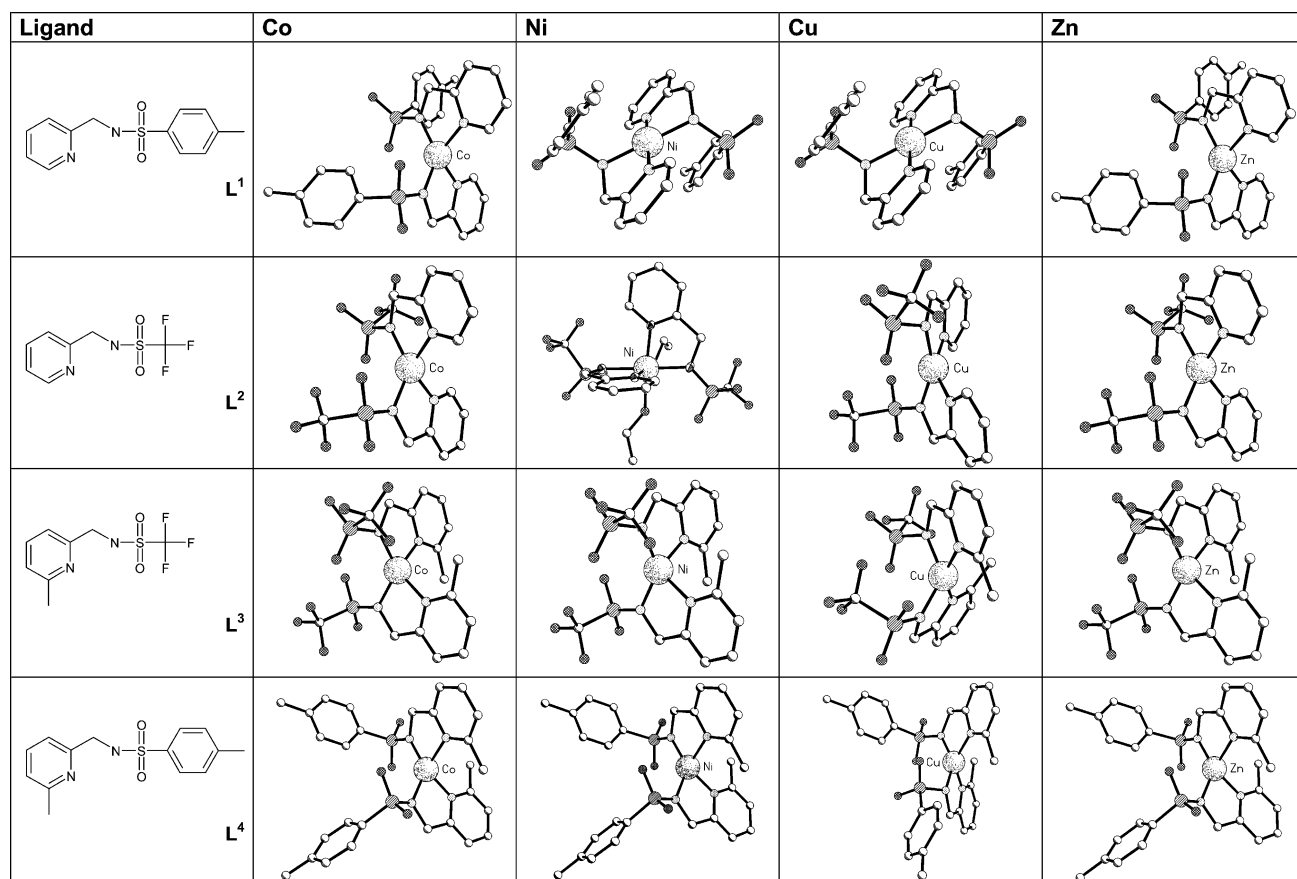
Fig. 1 View of the crystal structures (100 to 120 K) of the Co(II), Ni(II), Cu(II) and Zn(II) complexes of L^1–L^4, revealing distorted tetrahedral geometry except for [Cu(L^1)$_2$], [NiL^1] (square planar), and [Ni(L^2)$_2$(EtOH)$_2$] (octahedral).

L^4, the distorted tetrahedral arrangement that characterised zinc and cobalt complex formation is favoured. Finally, for Ni(II) complexes, once again complexes with L^3 and L^4 adopted distorted tetrahedral arrangements, while $[Ni(L^1)_2]$ was square planar and $[Ni(L^2)_2]$ took up an octahedral geometry, with two ethanol molecules cis-coordinated and the sulfonamide nitrogens trans-related.

Geometric parameters are summarised in Tables 2 and 3. Within the series of zinc and cobalt complexes, average bond lengths to the sulfonamide N were marginally longer with the more electron poor trifluoromethyl-substituted pair of complexes. At the same time, the M–Npy bond length was slightly longer for the complexes with the 6-methyl substituent. Bond lengths to pyridyl and sulfonamide nitrogens were in line with literature values for 4- or 5-coordinate zinc complexes.[28–31] For example, in the 2,2-bipyridylzinc complex of cyclohexane-1,2-diylbis(methanesulfonamide) the sulfonamide N–Zn bond length was 1.94 Å with a bpy–N–Zn length of 2.05 Å.[28] With the copper(II) complexes, average bond lengths were slightly longer for the square planar example. The X-ray structure of $[Cu(L^1)_2]$ has been reported independently at 293 K very recently;[32,33] structural details echo those reported herein. Overall, there is a remarkable constancy in the M–N bond lengths. This can be related to the fixed chelate bite angle, associated with each ligand. Thus, the intra-ligand N–M–N′ bond angles in the series average 83° and 82° for the set of zinc and cobalt complexes respectively (Table 3). This relatively constant bite angle is also found ($83 \pm 3°$) in the square planar and octahedral Ni(II) complexes.

There are two limiting geometries for four-coordinate complexes: square planar and tetrahedral. In order to quantify the deviation from these limits in the complexes examined here, a search of the CSD was undertaken examining all first row four-coordinate complexes with N and O donors only. In the April 2001 version, 284 of these were for zinc complexes. The geometry around the central ion is defined by six bond angles and these were obtained from the database. For a square planar complex, the sum of these angles is 720°; around a tetrahedron the sum is 656°. However, the sum itself is not a sufficient measure of geometry, because in the limiting case of the perfect tetrahedron each of the six angles needs to be identical, whilst for a square planar arrangement two of the angles have to be 180° and the remaining four are 90°. A measure of distortion is obtained by calculating the average deviation of all six angles; for a perfect tetrahedron this is zero and for a perfect square plane it is 40° $[(2 \times 60 + 4 \times 30)/6]$. A plot of the average angular deviation (y axis) versus the sum of the six angles is given for all of the CN = 4 first row transition metal complexes with N and O donors only in the CSD (Fig. 2). In this Figure, the copper complex of L^1 appears in the top right hand corner, whilst the copper complex of

L^2 possesses an angular deviation of close to 25°. The remaining two copper structures (sum of angles 665 to 670°), each of the zinc and cobalt complexes and the three tetracoordinate nickel complexes form a cluster around 18–20°. Once again, for the complexes examined here, the degree of distortion is primarily related to the 5-ring chelate bite angle of about 82° imposed by the ligand structure.

This method for analysing distortion from a regular polyhedron may be extended to related octahedral or trigonal bipyramidal structures. For the unique case of tetrahedral distortion, an alternative (1-D) analysis involves an examination of the dihedral angle between the two ML_2 planes, with limits at 90° and 0° for ideal tetrahedral and square planar geometry. This method has one advantage in giving the absolute configuration for chiral systems. Such an analysis has been carried out for the 16 structures defined herein. For each of the tetrahedrally distorted cobalt, nickel and zinc complexes, the deviation from the tetrahedral (90°) limit was not more than 10°. Distortion was more evident with the copper complexes; for $[Cu(L^2)_2]$ the dihedral angle was 45° whilst for $[Cu(L^3)_2]$ and $[Cu(L^4)_2]$, the values were 29 and 33° respectively. The 2-D plot shown in Fig. 2 intrinsically provides additional information. Tetragonal distortion of a square planar complex gives an angle sum of near to 720° and an angular distortion of $> 40°$; no cases were found for first row elements with O and N donors, only two examples with M–M (Cu/Cu and Co/Cu) bonding fall on this limit.

Absorption spectroscopy and cyclic voltammetry

Absorption spectra were recorded for each of the coloured complexes in acetonitrile solution at a 1 mM concentration when observing the d–d bands, and in more dilute solution when charge-transfer bands were also observed. For the Co(II) complexes, the absorption spectra were similar except for $[Co(L^4)_2]$, which was much more pale-coloured in the MeCN solution (Fig. 3). Molar absorption coefficients, ε, decreased in the sequence $[Co(L^2)_2] \ll [Co(L^1)_2] < [Co(L^3)_2] < [Co(L^4)_2]$. It is generally appreciated that visible transitions in tetrahedral cobalt(II) complexes are an order of magnitude more intense than for equivalent octahedral systems. Absorption spectra tend to be dominated by the $^4A_2 \rightarrow {}^4T_1(P)$ transition for tetrahedral systems, and $^4T_{1g}(F) \rightarrow {}^4T_{1g}(P)$ transition for octahedral examples. Fine structure is imposed by a number of transitions to doublet excited states, which gain intensity by spin–orbit coupling. Thus for $[Co(L^2)_2]$, the complex must be octahedral in solution, binding to two additional solvent molecules (viz. Fig. 1 for $[Ni(L^2)_2(EtOH)_2]$). Indeed, the reflectance spectra for each cobalt complex—obtained on crystalline samples—were more or less identical in intensity, supporting this idea.
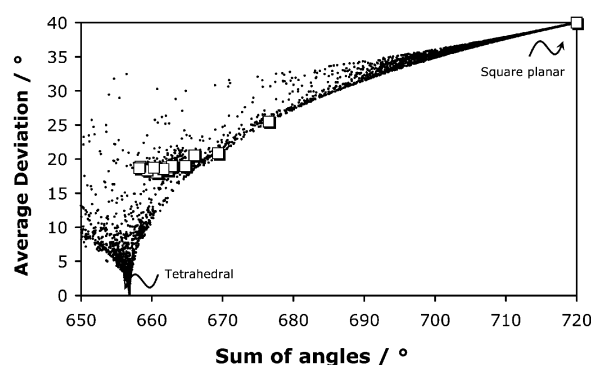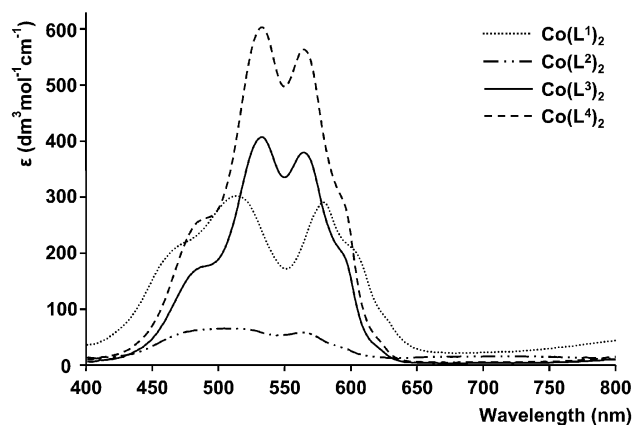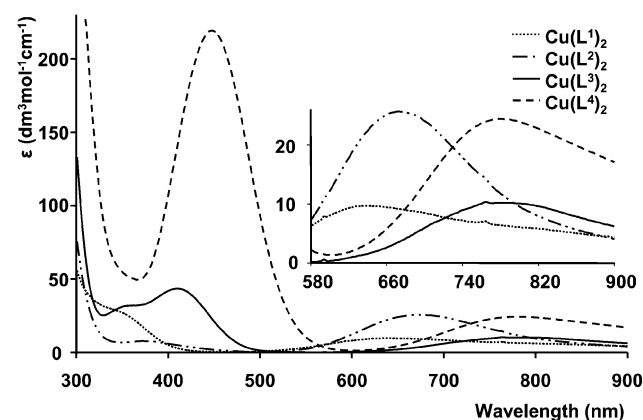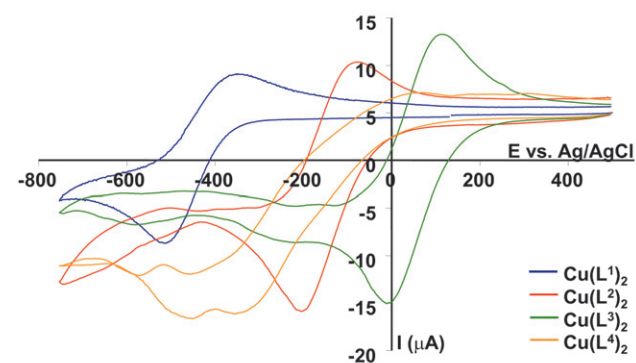

Fig. 2 Plot of the sum of the six bond angles (x axis) versus the average deviation of these angles for all 4-coordinate first row transition metal complexes involving N and O donors (CSD 2001). The complexes in this paper are represented by squares (see Table 3).

Fig. 3 Absorption spectra of neutral cobalt(II) complexes of L^1–L^4 (1 mM complex, (2 mM for L^2), MeCN).

Table 4 Selected absorption spectral data (MeCN, 295 K) for cobalt, nickel and copper(II) complexes (λ_{max}; ε/M^{-1} cm^{-1} in parentheses)

	Co(II)	Ni(II)	Cu(II)
L^1	513 (300), 579 (290)	insoluble	639 (70)
L^2	500 (45)	367 (50), 597 (3)	672 (230)
L^3	533 (400), 564 (380)	544 (190), 733 (50)	410 (405), 764 (70)
L^4	532 (580), 564 (540)	544 (70), 760 (30)	448 (2020), 784 (215)

Table 5 Selected ligand protonation and successive metal complex formation constants (298 K, $I = 0.1$ M NMe$_4$NO$_3$, 80% MeOH–20% H$_2$O)
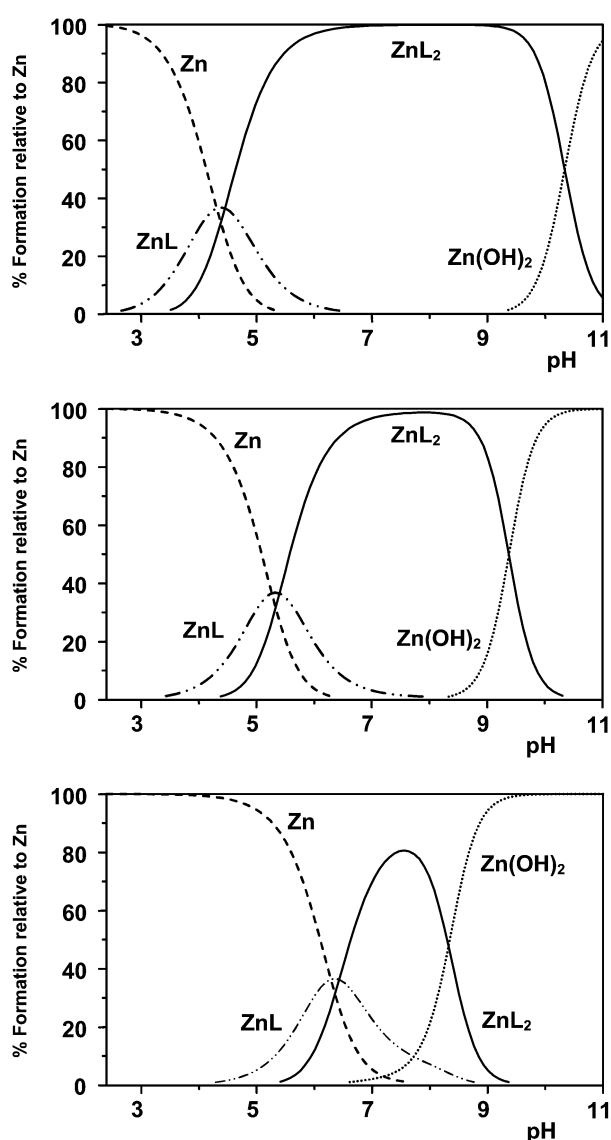
	log $K_1{}^a$	log K_2	log K_{ZnL}	log K_{ZnL_2}	log K_{CuL}	log K_{CuL_2}
L^1	12.23(6)	3.31(3)	7.66(6)	6.91(7)	11.40(5)	9.16(7)
L^2	7.51(3)	2.69(3)	5.25(5)^b	5.12(7)^b	6.74(5)	6.42(8)
L^3	7.61(3)	3.23(3)	^{c}	^{c}	6.26(4)	6.09(8)

^{a} Defining the successive protonation constants: $K_1 = [LH]/[L^-][H^+]$ and $K_2 = [LH_2{}^+]/[LH][H^+]$. ^{b} Values for Co complexes were: log K_{CoL} 5.11(6); log K_{CoL_2} 5.19(5). ^{c} Precipitation occurred under these conditions.

The tetrahedrally distorted copper complexes, [Cu(L^3)$_2$] and [Cu(L^4)$_2$], were lime-green and orange-brown in solution (Table 4 and Fig. 4), reflecting the influence of the relatively intense LMCT bands at 410 and 448 nm respectively. The portion of the d–d transition was shifted to the red in the sequence [Cu(L^1)$_2$] > [Cu(L^2)$_2$] > [Cu(L^3)$_2$] > [Cu(L^4)$_2$] associated with the increase in LFSE for square-planar complexes, with the more polarisable NTs ligand in L^1 affording the greatest crystal field splitting. The Cu^{II}/Cu^I redox couple was examined by cyclic voltammetry (MeCN, Bu$_4$NClO$_4$, 295 K) for each of the four copper complexes (Fig. 5). For the complexes lacking the 6-Me substituent, the $E_{\frac{1}{2}}$ values (vs. Ag/AgCl) were −430 [Cu(L^1)$_2$] and −137 mV ([Cu(L^2)$_2$]), reflecting the greater stabilisation of the copper(II) state in the tosylamide complex with square planar geometry and a large ligand field stabilisation energy (Table 4). The tetrahedrally distorted complex [Cu(L^3)$_2$] is much more readily reduced, $E_{\frac{1}{2}} = +55$ mV, consistent with the destabilisation of the Cu(II) state. In each of these cases, quasi-reversible behaviour was exhibited ($i_p \approx i_{a_i}$ $i_a \propto v^{1/2}$), whereas for the tetrahedrally distorted complex

[Cu(L^4)$_2$], more complex behaviour was noted with an apparent redox couple at ca. −240 mV.

Selected ligand protonation and metal complex formation constants: speciation at ambient pH

Equilibrium constants associated with stepwise protonation of the anionic ligands L^1–L^3 were measured by standard

Fig. 4 Absorption spectra of neutral copper(II) complexes of L^1–L^4, the inset highlights the position of the $^2E_{2g} \rightarrow {}^2T_{2g}$ transition.

Fig. 5 Cyclic voltammograms (295 K, 0.1 M Bu$_4$NClO$_4$, $v = 100$ mV s^{-1}) of the copper(II) complexes of L^1–L^4.

Fig. 6 Species distribution plots for Zn^{2+}/L^2: upper, 10 mM ligand, 1 mM Zn^{2+}; centre, 1 mM L^2, 0.1 μM Zn^{2+}; lower, 0.1 mM L^2, 0.1 μM Zn^{2+} (80% MeOH, 20% H$_2$O; 298 K; 0.1 M Me$_4$NNO$_3$). Plots at a fixed L/M ratio of 2 are given in the ESI.†
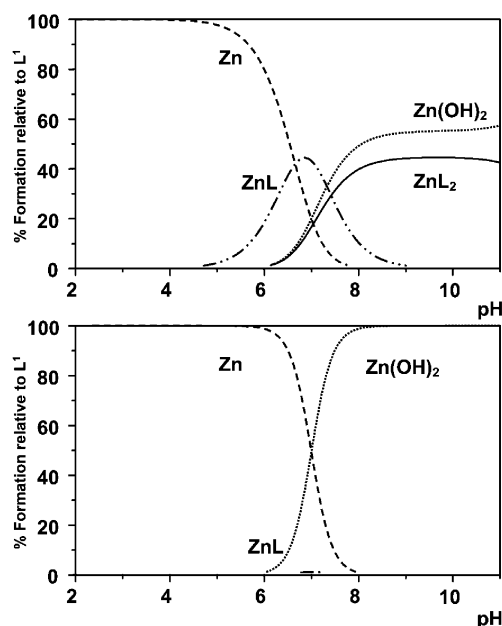
Fig. 7 Species distribution plots for Zn^{2+}/L^1: *upper*, 10 mM ligand, 1 mM Zn^{2+}; *lower*, 0.1 mM L^1, 10 μM Zn^{2+}.

pH-metric methods in 80% $MeOH/H_2O$, in a background of 0.1 M NMe_4NO_3. Data were corrected[24] to allow for the variation of the water dissociation constant at this solvent composition and were analysed using the programme HYPERQUAD.[23] The log K_1 values (Table 5) measured for L^2 and L^3 were 7.51 and 7.61 respectively, similar to the literature values for simple trifluoromethylsulfonamides.[19] The *p*-toluenesulfonyl analogue, L^1, possesses a much more basic sulfonamide N, log K_1 = 12.23, in line with data for related arylsulfonamides.[34] The pyridyl nitrogen is much less basic in each case, and the introduction of the 6-methyl substituent slightly enhances proton affinity (L^2 *vs.* L^3: log K_2 = 2.69 and 3.32). Thus, around ambient pH conditions, the ligands L^2 and L^3 exist as almost 50% of the monoanionic species.

Metal complex formation constants have been measured for Cu(II) and Zn(II) complexes of L^1–L^3, taking account of metal ion hydrolysis.[23] Separate titrations at 1:1 and 1:2 metal/ligand ratios were undertaken in order to measure both the ML and the ML_2 formation constants. The ligand L^2 formed slightly more stable complexes with copper than zinc, in accord with the Irving–Williams series,[35] although a direct comparison of the tetrahedrally distorted $Cu-L^3/Zn-L^3$ systems

is not possible here, owing to the insolubility of the zinc complex under the standard conditions used. The difference in stability of the copper and zinc complexes is much greater with L^1, as the copper complex in that case is square planar and the zinc is tetrahedral. The relative magnitude of the stepwise formation constants (log K_{ML} *vs.* log K_{ML_2}) for zinc, copper and cobalt was very similar, although there was no evidence for the positive cooperativity in formation of the ML_2 complex, that was apparently a feature of the behaviour of the related quinolylsulfonamides (*e.g.* Zinquin[5]). It should be noted that the analysis of the data reported in that case ("we conclude that that the 1:1 and 2:1 Zn/Zinquin complexes differ by at least two orders of magnitude"[5]) only gives a limit to the difference in values as no direct titrations were reported at 1:1 stoichiometry and there was no direct account taken of metal ion hydrolysis in the data analysis.

The harder trifluoromethylsulfonamide N favours binding to Cu(II) less than the more basic and softer tosylamide N in L^1. Hard donors—such as phosphinates—have previously been shown to disfavour binding to Zn^{2+} less than to Cu^{2+}, in related 4 or 5-coordinate aza-phosphinate complexes.[21] Furthermore, systems favouring tetrahedral coordination should also enhance the relative stability of Zn(II) compared to Cu(II), as the LFSE contribution is significantly diminished for Cu(II) when deviations from planarity or square pyramidal geometry occur.[13,14,22]

Using the data in Table 5, species distribution diagrams as a function of pH and M/L concentration may be obtained, in which the percentage of the insoluble metal hydroxide is calculated by extrapolation. Considering the Zn^{2+}/L^1 and L^2 systems (Figs. 6 and 7), the pH-dependent distribution of complex species has been calculated at fixed ligand concentrations of 10 mM, 1 mM and 0.1 mM, with varying $[Zn^{2+}]$ values. Distributions at a fixed 2:1 ligand to metal ratio are given in the ESI.† With the Zn^{2+}/L^2 system, a particular feature is that the $[Zn(L^2)_2]$ species predominates at ambient pH and even with $[L^2]_{tot}$ = 0.1 mM and $[Zn^{2+}]$ = 0.1 mM, more than 80% of all Zn bound species is $[Zn(L^2)_2]$. On the other hand, with the tosylamide ligand L^1 (log K_1 = 12.2) even at 10 mM $[L^1]_{tot}$ and 1 mM $[Zn^{2+}]_{tot}$, the major species at pH 7.4 is the metal hydroxide with significant $[ZnL^1]$ formed. At lower ligand concentrations, only a small percentage fraction of the $[ZnL^1]$ species is present. Given that L^2 and L^3 may be readily derivatised at C-6 or alpha to the sulfonamide N, these ligands offer some scope as the basis for Zn^{2+} probes in neutral aqueous media.

For the Cu(II)/L^1 system, exhibiting, as expected, the highest stepwise formation constants for any of the systems examined here, it is possible to vary the pH over the range 4 to 8 in order to control the relative proportion of $[CuL^1]$ and $[Cu(L^2)_2]$
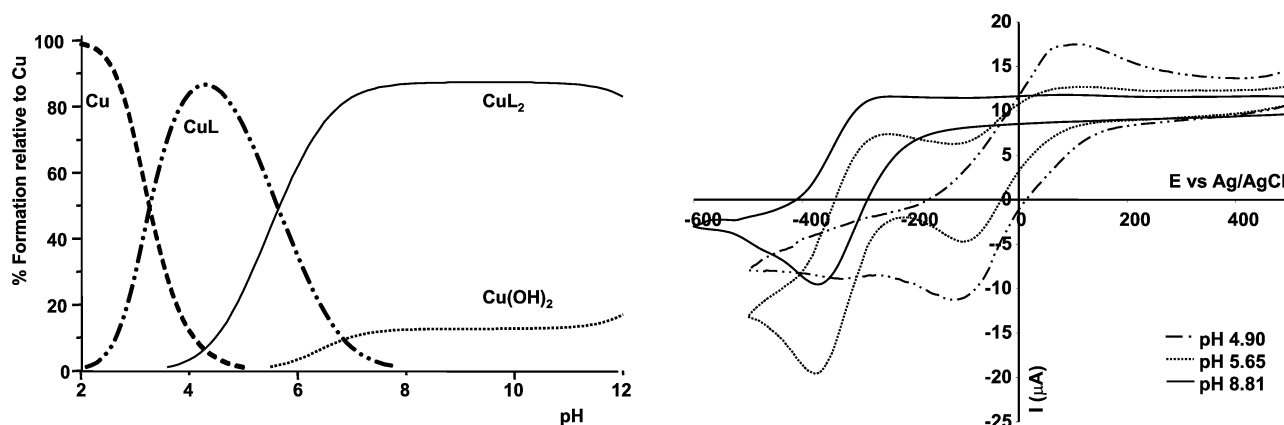

Fig. 8 *Left*: Species distribution plot for Cu^{2+}/L^1 (10 mM L^1, 5 mM Cu^{2+}, 298 K, 80% MeOH, 20% H_2O, 0.1 M NMe_4NO_3); *right*: cyclic voltammograms recorded under the same conditions at pH 4.9, 5.65 and 8.81 (v = 100 mV s^{-1}).

species (Fig. 8 *left*). Thus, for a ligand concentration of 10 mM (or 1 mM), at pH 5 the predominant species is [CuL^1], whereas at pH > 7, [Cu(L^2)$_2$] is the major species. With this in mind, cyclic voltammetry was used to examine the Cu(II)/Cu(I) redox couple as a function of pH (Fig. 8 *right*). At pH 4.9 (10 mM L^1; 5 mM Cu(CF$_3$SO$_3$)$_2$; 298 K; 0.1 M NMe$_4$NO$_3$, 80% MeOH/H$_2$O), the reversible wave observed at *ca.* −10 mV may be ascribed to [CuL^1], whereas at pH 8.8, the redox couple shifts to −315 mV and is associated with the square planar complex [Cu(L^2)$_2$]. At the intermediate pH value of 5.65, both species are present in nearly equal amounts, and the observation of separate redox waves for each species is consistent with the rate of electron transfer being faster than any associative ligand exchange process involving [CuL^1] and [Cu(L^2)$_2$]. Given that different redox active ML species may be observed simultaneously, for example using differential pulse voltammetry, and that their relative concentration is pH dependent, such work suggests that by immobilising ligands related to L^1 at an electrode surface, the selective detection and assay of a mixture of metal ions may be expedited using sensitive stripping voltammetric techniques.

In summary, ligands L^2 and L^3 are suitable basic ligand systems that form ML$_2$ complexes at ambient pH when the free zinc concentration is in the micro to nanomolar range. Suitable derivatives are therefore being evaluated allowing their integration into practicable luminescent or MRI probes.

References

1 R. J. P. Williams and J. J. R. Frausto da Silva, *Coord. Chem. Rev.*, 2000, **200–202**, 247.

2 D. W. Choi and J. Y. Koh, *Annu. Rev. Neurosci.*, 1998, **21**, 347.

3 L. M. T. Canzoniero, D. M. Turetsky and D. W. Choi, *J. Neurosci.*, 1999, **19**, RC31.

4 J. H. Weiss, S. L. Sensi and J. Y. Koh, *Trends Pharm. Sci.*, 2000, **21**, 395.

5 C. J. Fahrni and T. V. O'Halloran, *J. Am. Chem. Soc.*, 1999, **121**, 11 448.

6 K. R. Gee, Z.-L. Zhou, W.-J. Qian and R. Kennedy, *J. Am. Chem. Soc.*, 2002, **124**, 776.

7 T. Hirano, K. Kikuchi, Y. Urano, T. Higuchi and T. Nagano, *Angew. Chem., Int. Ed.*, 2000, **39**, 1052; T. Hirano, K. Kikuchi, Y. Urano, T. Higuchi and T. Nagano, *J. Am. Chem. Soc.*, 2000, **122**, 12 399.

8 G. K. Walkup, S. C. Burdette, S. J. Lippard and R. Y. Tsien, *J. Am. Chem. Soc.*, 2000, **122**, 5644.

9 P. D. Zalewski, S. H. Millard, I. J. Forbes, O. Kapaniris, A. Slavotinek, W. H. Betts, A. D. Ward, S. F. Lincoln and I. Mahadevan, *J. Histochem. Cytochem.*, 1994, **42**, 877.

10 W. D. Qian, C. A. Aspinwall, M. A. Battiste and R. T. Kennedy, *Anal. Chem.*, 2000, **72**, 711.

11 O. Reany, T. Gunnlaugsson and D. Parker, *J. Chem. Soc., Perkin Trans. 2*, 2000, 1819.

12 Y. Hitomi, C. E. Outten and T. V. O'Halloran, *J. Am. Chem. Soc.*, 2001, **123**, 8614.

13 C. D. Edlin, D. Parker, J. J. B. Perry, C. Chartroux and K. Gloe, *New J. Chem.*, 1999, **23**, 819.

14 G. B. Bates, D. Parker and P. A. Tasker, *J. Chem. Soc., Perkin Trans. 2*, 1996, 1117.

15 J. M. Berg and Y. Shi, *Science*, 1996, **271**, 1081.

16 T. Koike, E. Kimura, I. Nakamura, Y. Hashimoto and M. Shiro, *J. Am. Chem. Soc.*, 1992, **114**, 7338; U. Hartmann and H. Vahrenkamp, *Inorg. Chem.*, 1991, **30**, 4676.

17 E. E. Chufan, S. Garcia-Granda, M. R. Diaz, J. Borras and J. C. Pedregosa, *J. Coord. Chem.*, 2001, **54**, 303.

18 C. T. Supuran and A. Scozzafava, *Eur. J. Med. Chem.*, 2000, **35**, 867.

19 K. Hakansson and A. Liljas, *FEBS Lett.*, 1994, **350**, 319.

20 D. Elbaum, S. K. Nair, M. W. Patcham, R. B. Thompson and D. W. Christianson, *J. Am. Chem. Soc.*, 1996, **118**, 8381.

21 G. B. Bates, E. Cole, R. Kataky and D. Parker, *J. Chem. Soc., Dalton Trans.*, 1996, 2693.

22 G. B. Bates and D. Parker, *J. Chem. Soc., Perkin Trans. 2*, 1996, 1109.

23 P. Gans, A. Sabatini and A. Vacca, *Talanta*, 1996, **43**, 1739; L. Alderighi, P. Gans, A. Ienco, D. Peters, A. Sabatini and A. Vacca, *Coord. Chem. Rev.*, 1999, **184**, 311; P. Gans, A. Sabatini and A. Vacca, *J. Chem. Soc., Dalton Trans.*, 1985, 1195; P. Gans, A. Sabatini and A. Vacca, *Talanta*, 1996, **43**, 1739.

24 S. Rondini, P. R. Mussini and T. Mussini, *Pure Appl. Chem.*, 1987, **59**, 1549.

25 SHELXTL version 6.12, Bruker AXS, Madison, Wisconsin, USA, 2001.

26 O. Fuentes and W. W. Pandler, *J. Org. Chem.*, 1975, **40**, 1210.

27 R. D. Shannon, *Acta Crystallogr., Sect. C*, 1976, **32**, 751.

28 S. E. Denmark, S. P. O'Connor and S. R. Wilson, *Angew. Chem., Int. Ed.*, 1998, **37**, 1149.

29 S. Z. Haider, K. M. A. Malik, M. B. Hursthouse and S. Das, *Acta Crystallogr., Sect. C*, 1984, **40**, 1147.

30 U. Hartmann and H. Vahrenkamp, *Z. Naturforsch. B*, 1994, **49**, 1725.

31 S. L. Sumalan, J. Casanova, G. Alzuet, J. Borras, A. Castineiras and C. T. Supuran, *J. Inorg. Biochem.*, 1996, **62**, 31.

32 L. Gutierrez, G. Alzuet, J. A. Real, J. Cano, J. Borras and A. Castineiras, *Inorg. Chem.*, 2000, **39**, 3608.

33 L. Gutierrez, G. Alzuet, J. Borras, M. Liu-Gonzalez, F. Sanz and A. Castineiras, *Polyhedron*, 2001, **20**, 703.

34 B. Nyasse, L. Grehn, U. Ragnarsson, H. L. S. Maia, L. S. Monteiro, I. Leito, I. Koppel and J. Koppel, *J. Chem. Soc., Perkin Trans. 1*, 1995, 2025.

35 H. M. N. H. Irving and R. J. P. Williams, *J. Chem. Soc.*, 1953, 3192.